# Fast proton-hydrogen charge exchange reaction at small scattering angles

P. S. Vinitsky* and Yu. V. Popov
*Nuclear Physics Institute, Moscow State University, Moscow 119899, Russia*

O. Chuluunbaatar
*Joint Institute of Nuclear Research, Dubna, Moscow Region 141980, Russia*
(Received 11 August 2004; published 7 January 2005)

The process in which a fast passing proton captures an electron from a hydrogen atom and scatters at small angles is considered. In contrast to previous calculations within the peaking approximation the numerical calculations of the second Born as well as second Born-Faddeev diagrams are presented. The results of calculations are compared with the experimental data obtained at 2.8 and 5.0 MeV impact energy. It is shown that numerical second Born calculations give quite different results from that in the peaking approximation. In particular, the role of the *pp* interaction is rather noticeable. On the other hand, the second Born-Faddeev numerical calculations clearly demonstrate the important role of distortion of plane waves.

DOI: 10.1103/PhysRevA.71.012706 PACS number(s): 34.70.+e, 02.60.Jh

## I. INTRODUCTION

The processes in which a fast ion captures one or several electrons colliding with an atomic target have been studied for a long time and their theory has been well established [1,2]. However, in precise coincidence experiments on the helium atom, where the fast proton captures the electron simultaneously ionizing a recoil ion all independent kinematical characteristics of all the final particles have been measured, with the use of a unique COLTRIMS technique [3]. The scattering angle of helium has been scanned in the range 0.1–0.5 mrad and the proton energy has been varied in the range $E_p = 0.15-1.4$ MeV.

The experimentalists suggested that such reactions could be used as a test for the atomic ground state wave function and this idea has become a subject of controversy [4]. Actually, the behavior of the single differential cross section (SDCS) in the angular range 0.1–0.3 mrad depends on the choice of the helium ground state wave function because of the domination of the direct capture mechanism. But preliminary calculations showed that the contribution of other reaction mechanisms, including double scattering, is substantial. Thus a problem of the most extensive and precise calculations of different reaction mechanisms arises. To our knowledge, no such calculations have been performed for a helium target. Moreover, the uncertainty related to the helium wave function, which is not known exactly, strongly complicates the analysis of the role of double scattering. In view of these facts it is natural to start by considering the simpler charge exchange reaction

$$p + \mathrm{H}(1s) \to \mathrm{H}(1s) + p', \tag{1}$$

in which case the atomic wave function is known exactly. Such an approach allows us to develop an accurate calculation scheme to evaluate the contributions from different reaction mechanisms. Measurements of the SDCS of reaction (1) at projectile energies of the order of a few MeV and at proton scattering angles in the range $\theta_p \in [0, 0.6]$ mrad were carried out by Vogt *et al.* [5].

Let us label the projectile proton by index 1 and the target proton by index 2 and write down basic quantum mechanical equations to calculate the amplitude of reaction (1). The Hamiltonian of the system reads

$$H = T_1 + T_2 + T_e + W = H_0 + W, \tag{2}$$

where $W = V_{e1} + V_{e2} + V_{12}$ is the total interaction potential. The exact amplitude of reaction (1) is given by

$$\mathcal{T} = \langle \phi_f | (W - V_{e2} - \omega) | \phi_i \rangle + \langle \phi_f | (W - V_{e1} - \omega') \mathcal{G}(E) (W - V_{e2} - \omega) | \phi_i \rangle, \tag{3}$$

where $\mathcal{G}(E) = (E - H + i0)^{-1}$ is the full Green's function of the system, and $\omega, \omega'$ are the distorting potentials. In Eq. (3) the initial and final states satisfy the respective equations

$$[E - H_0 - V_{e2} - \omega] | \phi_i \rangle = 0,$$

$$[E - H_0 - V_{e1} - \omega'] | \phi_f \rangle = 0. \tag{4}$$

All calculation schemes for the amplitude $\mathcal{T}$ are based on different approximations to Eq. (3). The first term denotes the single-collision mechanisms and can be called the first Born approximation (B1). In this case the choice of the distorting potential $\omega$ depends on the particulars of the approximation as well as on the possibility of carrying out the complex numerical calculations. The continuum distorted wave (CDW) models [6–8], where in the initial and final states the Coulomb interaction between the proton and $(ep)$ pair fragments is taken into account, have been widely used.

If we put $\mathcal{G}(E) = \mathcal{G}_0(E)$ in Eq. (3), then one considers the mechanisms of double scattering including the distorted waves as well. The sum of the first and second terms is called the second Born approximation (B2). In 1927 Thomas [9], using only classical treatment, showed the importance of double electron scattering. It is important to mention the work [10] on quantum treatment of double-scattering mechanisms. It has become clear that the contribution of particular double-scattering mechanisms of particles in the intermedi-

*Electronic address: vinitsky@srd.sinp.msu.ru

 

ate states is comparable with and sometimes much bigger than that of the B1 approximation in certain angular domains. Thus a problem of numerical calculations of B2 matrix elements arises. These terms are described by sixfold integrals.

As far as we know, the first numerical calculations of B2 integrals without partial decompositions were performed by Simony and McGuire [11] using the technique of the Lewis integrals that is widely applied in high-energy physics for calculating Feynman diagrams. However, they calculate only the so-called electronic part of the total interaction potential $W$, ignoring the $pp$ interaction $V_{12}$. Such a choice is based on the conclusion that all the B2 terms which include the $pp$ potential cancel each other. This conclusion, in turn, follows from the so-called peaking approximation [12,13], which should be valid at high collision energies, however high they could be. At the energies of actual experiments [5] the peaking approximation might be too crude.

Reaction (1) is a fundamental example of the three-body problem, and such problems should be considered in the context of Faddeev equations (see, for example, the monograph [14]). The step-by-step Born-Faddeev approximations (B1F, B2F) can be derived directly from Eqs. (2) and (3) using some transformations of full Green's functions. The nonrelativistic diagram method [15] is also effective. In such an approach, instead of the two-body potentials the two-body off-shell scattering amplitudes appear in matrix elements. In fact, this replacement allows us to take into account some multiple scattering (distortion) and to investigate its contribution to the full amplitude (3). For the first time such estimations were presented in [16] and the approximate B2F calculations as well as comparison with experimental data were given in [17] (B2F is referred to as FWL there). The FWL model employs both the peaking approximation and an approximation of the two-body off-shell amplitude, using its small deviation from the on-shell one, which is typical of the eikonal approximation widely utilized in calculations of capture reactions (see also the very recent publication on this subject [19]).

In this work the results of complex numerical B2 and B2F calculations for reaction (1) are presented. It is shown that the results of the precise numerical calculations differ considerably from those of the peaking approximation. Precise B1F calculations and first-order FWL (FWL1) calculations were also carried out by us. It follows from the comparison that the FWL approximation is rather crude at moderate energies. The results of the numerical B2F calculations are also presented. In our approach the $(pp)$ amplitude is taken exactly by using the Schwinger representation [21], while the $(ep)$ amplitude is evaluated using the closure approximation, which takes into account the averaged contribution of intermediate $(ep)$ pair excitations. Besides that, we apply another technique of calculation of complex integrals based on the Laplace transform.

In the present calculations we neglect all the terms of the same order with ratios of both the electron mass and the transferred momentum to the masses of heavy particles, as is generally accepted. In other words, the target nucleus (the proton) is assumed to be at rest in the laboratory system during the reaction. Therefore we neglect the nuclear exchange processes too. Atomic units $m_e=e=\hbar=1$ are used throughout the paper.

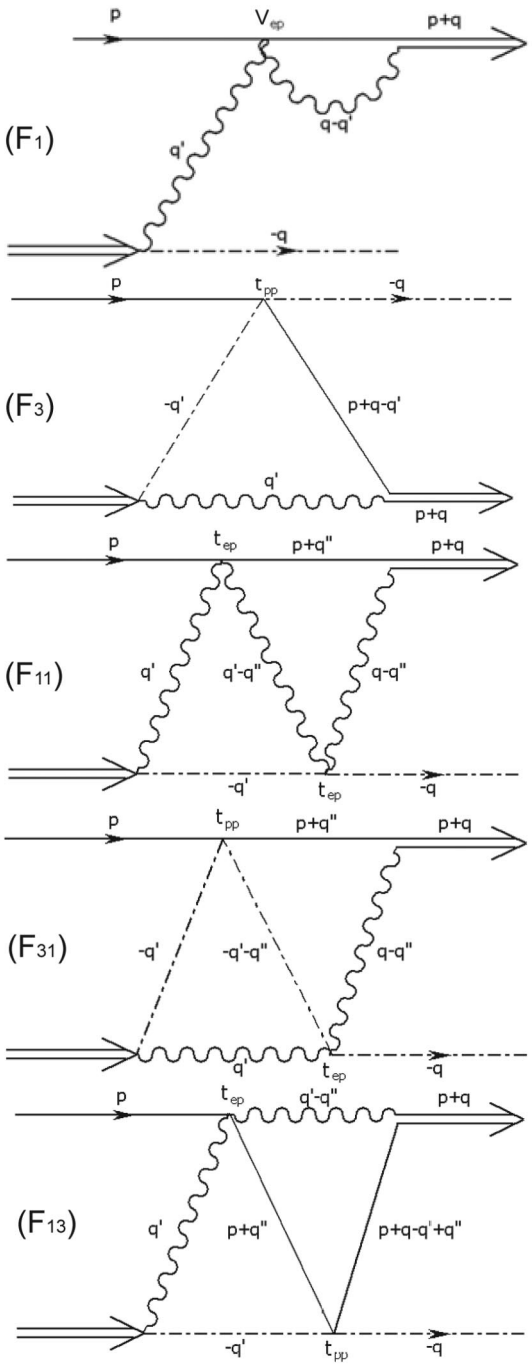


FIG. 1. First- and second-order Born-Faddeev diagrams for reaction (1). Solid line corresponds to the fast proton, wavy line to the electron, chain line to the slow nucleus, and the array to hydrogen.

## II. THEORY

Let us denote the projectile momentum by $\vec{p}$, the final-state hydrogen momentum by $\vec{p}_H$, and the recoil-ion momentum by $\vec{K}$. Therefore, we can introduce a transferred momentum $\vec{q}=\vec{p}_H-\vec{p}$. The momentum and energy conservation laws

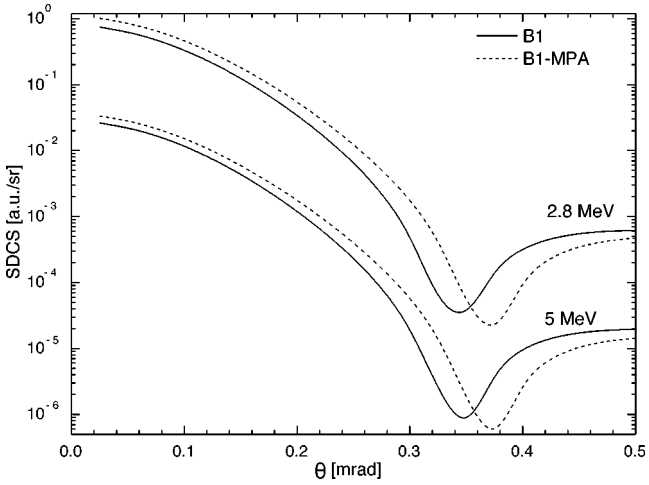


FIG. 2. Differential cross sections for $1s \rightarrow 1s$ capture in 2.8 and 5.0 MeV proton-hydrogen collisions vs the scattering angle in the laboratory system. Results of B1 (solid line) and B1-MPA (dashed line) calculations are compared.

in the laboratory system thus assume the respective forms

$$\vec{K} = -\vec{q},$$

$$E_0^{\mathrm{H}} + \frac{p^2}{2m} = \frac{(\vec{p}+\vec{q})^2}{2(m+1)} + \frac{q^2}{2m} + E_0^{\mathrm{H}}. \tag{5}$$

In Eq. (5) $m=1836.15$ is the proton mass, and $E_0^{\mathrm{H}}=-0.5$ is the hydrogen ground-state energy. Choosing the direction of the proton velocity $\vec{v}_p=\vec{p}/m$ along the $z$ axis one gets $q_\perp = mv_p \sin\theta_p \approx mv_p\theta_p$ in the case of small $\theta_p$.

A peculiarity of the scattering at small angles is that the transferred momentum $q$ is much smaller than the proton (nucleus) mass. It allows one to assume the nucleus to be at rest during the reaction, i.e., to neglect $q^2/2m$ in Eq. (5). Under this assumption, from Eq. (5) it follows that

$$q_z = \frac{v_p}{2}. \tag{6}$$

And even if $v_p \lesssim 20$ a.u. and $m\theta_p$ is several a.u., the inequality $q^2/2m \ll 1$ holds true.

The SDCS for the scattering of hydrogen in the direction specified by the solid angle $\Omega$ in the laboratory system is given by

$$\frac{d\sigma}{d\Omega} = \frac{m^2}{(2\pi)^2}|\mathcal{T}|^2, \tag{7}$$

where $\mathcal{T}$ is the capture process amplitude

$$\mathcal{T} = \langle \varphi_{2e}, \vec{p}|(V_{1e}+V_{12})|\Psi\rangle. \tag{8}$$

In Eq. (8) $|\varphi_{2e}\rangle$ is the hydrogen initial ground state and $|\Psi\rangle$ is the total wave function of the system. Let us present the total wave function as $|\Psi\rangle = |\psi_{1e}\rangle + |\psi_{2e}\rangle + |\psi_{12}\rangle$ and for its components we write down a system of Faddeev equations:

$$|\psi_{1e}\rangle = \mathcal{G}_0^+ t_{1e}[|\psi_{2e}\rangle + |\psi_{12}\rangle] + |\varphi_{1e}(\vec{p_H}), \vec{K}\rangle,$$

$$|\psi_{2e}\rangle = \mathcal{G}_0^+ t_{2e}[|\psi_{1e}\rangle + |\psi_{12}\rangle],$$

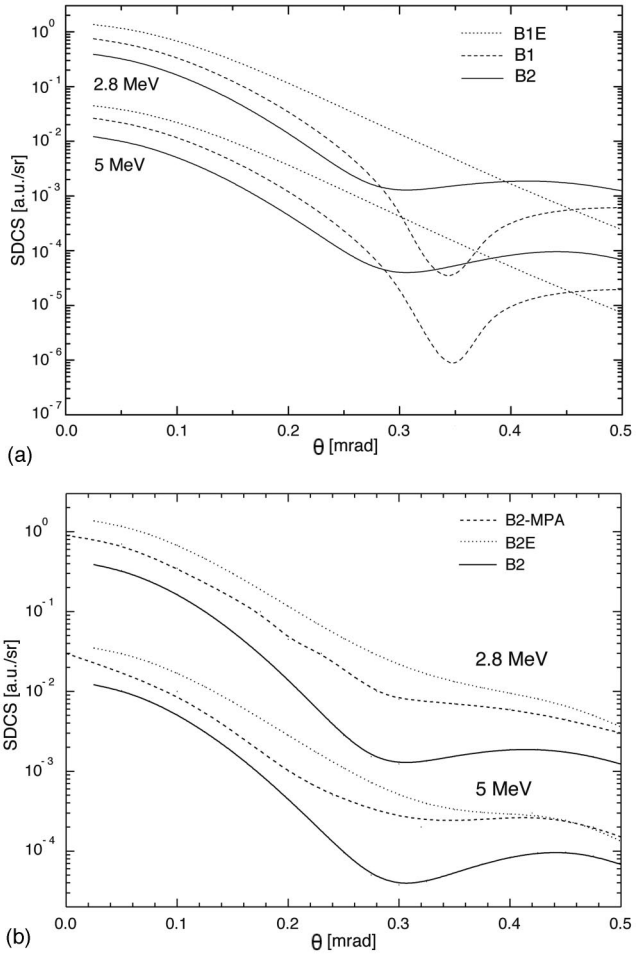


FIG. 3. Differential cross sections for $1s \rightarrow 1s$ capture in 2.8 and 5.0 MeV proton-hydrogen collisions vs the scattering angle in the laboratory system. Results of the BK term (17) (B1E, dotted line), B1 (dashed line), and B2 (solid line) calculations (upper panel), as well as B2 (solid line), B2-MPA (dashed line, Ref. [18]), and B2E (dotted line) calculations (lower panel) are compared.

$$|\psi_{12}\rangle = \mathcal{G}_0^+ t_{12}[|\psi_{1e}\rangle + |\psi_{2e}\rangle]. \tag{9}$$

Using the well-known operator identity $t = V + V\mathcal{G}_0^+ t$ one finds the amplitude of reaction (1):

$$\mathcal{T} = \langle \varphi_{2e}, \vec{p}|V_{1e} + t_{12} + t_{12}\mathcal{G}_0^+ t_{2e} + t_{1e}\mathcal{G}_0^+ t_{12} + t_{1e}\mathcal{G}_0^+ t_{2e} + \cdots |\varphi_{1e}(\vec{p_H}), \vec{K}\rangle. \tag{10}$$

In this work we consider series (10) up to the second-order terms (B2F). For the sake of visualization we present it in the form of five nonrelativistic diagrams (see Fig. 1). Let us denote them as $F_1$, $F_3$, $F_{11}$, $F_{13}$, and $F_{31}$, where the $(ep)$ scattering is labeled by 1 and the $(pp)$ scattering by 3.

Let us consider the first-order diagrams. The $F_1$ diagram represents the direct capture process [the first-order Brinkman-Kramers (BK) term] and assumes the form

$$F_1 = -\frac{4\sqrt{\pi}}{1+(\vec{v}_p - \vec{q})^2}\varphi_0(q), \tag{11}$$

where $\varphi_0(\vec{q}) = 8\sqrt{\pi}/(1+q^2)^2$ is the hydrogen ground-state wave function in the momentum space.

The triangular diagram $F_3$ corresponds to the process of proton-nucleus (proton) scattering and it has the following integral expression:

$$F_3 = \int \frac{d^3\vec{q}'}{(2\pi)^3}\varphi_0(q')t_{pp}\left(\frac{\vec{p}+\vec{q}'}{2},\frac{\vec{p}-\vec{q}'}{2}+\vec{q};\frac{p^2}{4m} + E_0^{\mathrm{H}} + \frac{\vec{v}_p\vec{q}'}{2} - \frac{q'^2}{2} + i0\right)\varphi_0(\vec{v}_p - \vec{q}'). \quad (12)$$

The arguments of the scattering amplitude are the relative incoming and outgoing momenta and the relative energy of a pair.

Then there are three second-order diagrams of the Born-Faddeev approximation, involving $(ep)$ scattering and $(pp)$ scattering processes in the intermediate state. The diagrams $F_{11}$, $F_{13}$, and $F_{31}$ assume the integral form:

$$F_{11} = \int \frac{d^3q'}{(2\pi)^3}\int \frac{d^3q''}{(2\pi)^3}t_{ep}\left(\vec{v}_p - \vec{q}', \vec{v}_p - \vec{q}' + \vec{q}'';E_0^{\mathrm{H}} + \frac{v_p^2}{2} - \vec{v}_p\vec{q}' + i0\right)\frac{\varphi_0(q')\varphi_0(\vec{v}_p + \vec{q}'' - \vec{q})}{E_0^{\mathrm{H}} - \vec{v}_p\vec{q}'' - (\vec{q}' - \vec{q}'')^2/2 + i0} \times t_{ep}(\vec{q}'' - \vec{q}', \vec{q}'' - \vec{q};E_0^{\mathrm{H}} - \vec{v}_p\vec{q}'' + i0), \quad (13)$$

$$F_{13} = \int \frac{d^3q'}{(2\pi)^3}\int \frac{d^3q''}{(2\pi)^3}t_{ep}\left(\vec{v}_p - \vec{q}', \vec{v}_p - \vec{q}' + \vec{q}'';E_0^{\mathrm{H}} + \frac{v_p^2}{2} - \vec{v}_p\vec{q}' + i0\right)\frac{\varphi_0(q')\varphi_0(\vec{v}_p + \vec{q}'' - \vec{q}')}{E_0^{\mathrm{H}} - \vec{v}_p\vec{q}'' - (\vec{q}' - \vec{q}'')^2/2 + i0} \times t_{pp}\left(\frac{\vec{p}+\vec{q}''+\vec{q}'}{2},\frac{\vec{p}+\vec{q}''-\vec{q}'}{2};E_0^{\mathrm{H}} + \frac{p^2}{4m} - \frac{(\vec{q}' - \vec{q}'')^2}{2} + i0\right), \quad (14)$$

$$F_{31} = \int \frac{d^3q'}{(2\pi)^3}\int \frac{d^3q''}{(2\pi)^3}t_{pp}\left(\frac{\vec{p}-\vec{q}'}{2},\frac{\vec{p}+2\vec{q}''-\vec{q}'}{2};E_0^{\mathrm{H}} + \frac{p^2}{4m} - \frac{\vec{q}'^2}{2} - \frac{\vec{v}_p\vec{q}'}{2} + i0\right)\frac{\varphi_0(q')\varphi_0(\vec{v}_p + \vec{q}'' - \vec{q})}{E_0^{\mathrm{H}} - \vec{v}_p\vec{q}'' - \vec{q}'^2/2 + i0} t_{ep}(\vec{q}', \vec{q}'' - \vec{q};E_0^{\mathrm{H}} - \vec{v}_p\vec{q}'' + i0). \quad (15)$$

Each two-body amplitude $t_{ij}$ can be presented as the sum

$$t_{ij} = v_{ij} + v_{ij}\mathcal{G}_0^+ t_{ij}, \quad (16)$$

where $\mathcal{G}_0^+$ is the free three-body Green's function. If in the functions $F_\alpha$ $(F_{\alpha\beta})$ the amplitudes $t_{ij}$ are substituted by the potentials $v_{ij}$ (in $F_3$ right up to the second order) one can obtain the B2 result. For example,

$$A_1 \equiv F_1 = -\frac{4\sqrt{\pi}}{1 + (\vec{v}_p - \vec{q})^2}\varphi_0(q), \quad (17)$$

$$A_3 = 4\pi\int \frac{d^3\vec{q}'}{(2\pi)^3}\frac{\varphi_0(q')\varphi_0(\vec{v}_p - \vec{q}')}{(\vec{q} - \vec{q}')^2}, \quad (18)$$

$$\mathrm{B2} = [A_1 + A_3 + A_{11} + A_{31} + A_{13} + A_{33}], \quad (19)$$

where $A_i$ $(i=1,3)$ and $A_{ij}$ $(i,j=1,3)$ are, respectively, the first- and second-order terms of the Born series.

Our definitions differ from those of Alston [17]. To avoid confusion we present below the table of correspondence:

$$\mathrm{B1E} = A_1 \rightarrow A_{B1} \quad [\text{Alston, Eq. (20)}],$$

$$\mathrm{B1} = A_1 + A_3 \rightarrow A_{B1} + \langle\Phi_f|V_{PT}|\Phi_i\rangle \quad (\text{Alston}),$$

$$\mathrm{B2} = A_1 + A_3 + A_{11} + A_{31} + A_{13} + A_{33} \rightarrow \langle\Phi_f|\mathcal{T}^{(2)}_{Born}|\Phi_i\rangle \quad [\text{Alston, Eq. (11)}],$$

$$\mathrm{B2E} = A_1 + A_{11} \rightarrow A_{B1} + \langle\Phi_f|V_{Te}G_0^+(E)V_{Pe}|\Phi_i\rangle \quad (\text{Alston}),$$

$$\mathrm{B1F} = A_1 + F_3 \rightarrow A_{B1} + A_n^{(1)} \quad [\text{Alston, Eq. (24)}],$$

$$\mathrm{B2F} = A_1 + F_3 + F_{11} + F_{13} + F_{31} \rightarrow \langle\Phi_f|\mathcal{T}^{(2)}_R|\Phi_i\rangle \quad [\text{Alston, Eq. (4)}].$$

## III. RESULTS AND DISCUSSION

### A. First Born approximation

Usually in the literature the term $A_3$ is calculated in the so-called peaking approximation [12,13]. It is assumed that the regions of maxima of the function $\varphi_0$ mainly contribute to the integral (18). Since there are two such regions one introduces the multiple-peaking approximation (MPA) [18]. Using the precise numerical calculation of the integral (18) (details are presented in Appendix A), it is interesting to compare the B1 and B1-MPA results in a range of small scattering angles. As it follows from Fig. 2, where this comparison is presented, the difference between B1 and B1-MPA results is considerable. The convergence of the B1-MPA results to those of the B1 is extremely slow and it was found that even at $v_p=20$ the relative difference between the results is quite noticeable in the angular region $\theta_p \sim 0°$.

### B. Second Born approximation

The results of numerical B2 calculations for reaction (1) are shown in Figs. 3–5. The total contribution of the diagrams $A_{11}$, $A_{13}$, $A_{31}$, and $A_{33}$ is considerable in the whole angular region, and the processes of double collision play a significant role at the angles $\theta_p=0.3-0.5$ (see upper panel of Fig. 3). For numerical calculations the dimensions of the integrals $A_{ij}$ (see Appendix B) were reduced.

Calculations in the B2-MPA approximation [12,13,17,18] exhibit another tendency: the total contribution of the diagrams $(A_3+A_{13}+A_{31}+A_{33})$, involving the proton-nuclear interaction, tends to zero at asymptotically high $v_p$. However, this conclusion does not follow from the results of the

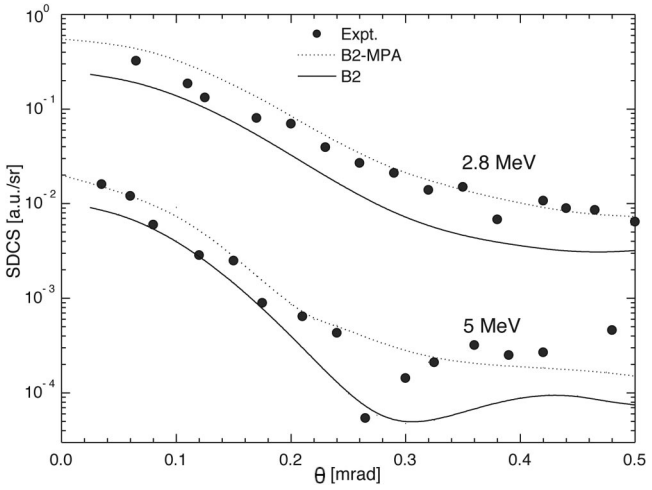


FIG. 4. Differential cross sections for $1s \rightarrow 1s$ capture in 2.8 and 5.0 MeV proton-hydrogen collisions vs the scattering angle in the laboratory system. Results of B2 (solid line) and B2-MPA (dotted line, Ref. [18]) calculations are compared with the experimental data of Vogt (Ref. [5]). The theoretical results have been convoluted with the beam profiles.

present numerical calculations. Figure 3 (lower panel) shows the calculation only of the electronic part of the interaction (B2E=$A_1+A_{11}$ diagrams) for the experimental velocities $v_p$ =10.6 and 14.2 a.u. It can be seen that the contribution of the proton-nuclear interaction is significant everywhere.

Comparison between exact numerical and MPA calculations of the B2 terms [18] is presented in Fig. 3 (lower panel). The following feature should be noticed: the B2-MPA calculation approaches the precise B2E calculation at large angles. It is interesting to compare the B2 results with experimental data. This comparison is presented in Fig. 4. To compare with experiment, the theoretical results were convoluted with the beam profile [5] (it is important to note that the theoretical results in Figures 2, 3, 5, 6, and 8 are presented without convolution). The convolution procedure strongly smooths the gap observed at $\theta \sim 0.3$ mrad. The difference between the numerical calculations and experimental data indicates the role of distorting factors, which is related to the fact that instead of the potentials the amplitudes are taken into account.

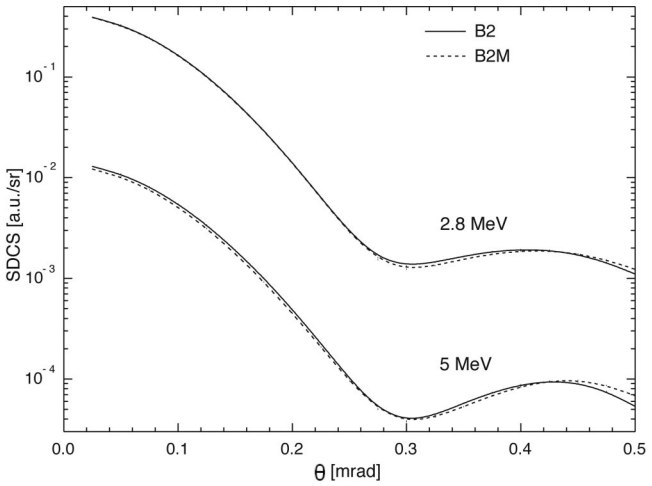


FIG. 5. Contribution of the recoil-ion motion (B2M, dashed line) to the differential cross section of the reaction (1) in comparison with B2 calculations.

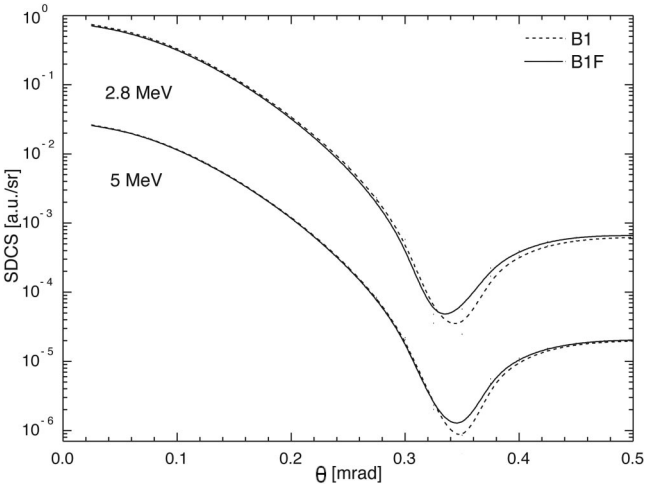


FIG. 6. Differential cross sections of reaction (1). Results of B1F (solid line) and B1 (dashed line) calculations are presented.

The precise B2M calculations including the recoil-ion motion (i.e., we leave in B2 all terms proportional to $1/m$) are also performed in Fig. 5 and the correctness of the hypothesis that the nucleus can be considered at rest is shown.

### C. Born-Faddeev approximation

Let $|\chi(\vec{p})\rangle$ be a solution of the two-body Schrödinger equation with the potential $v$. It is easy to show that $v|\chi(\vec{p})\rangle = t|\vec{p}\rangle$, i.e., the presence of amplitudes in the diagrams $F_i$ and $F_{ij}$ amounts to the account for the Coulomb distortion of the plane waves in intermediate states. This statement reflects the fact that the distorting potentials $\omega$ and $\omega'$ sometimes are used in Eq. (3) if the full Green's function is replaced by the free one. These potentials play no role in the exact equation, but in its approximate forms they can be important.

Let us compare the B1 and B1F results, when in the internuclear term $(A_3 \rightarrow F_3)$ we substitute $V_{pp} \rightarrow t_{pp}$. The Schwinger representation of the $t_{pp}$ amplitude is used to calculate numerically the $F_3$ diagram,

$$t_{pp}(\vec{p},\vec{p}';E) = 4\pi\left[\frac{1}{(\vec{p}-\vec{p}')^2} - i\eta I(\vec{p},\vec{p}';E)\right], \quad \eta = \frac{1}{\sqrt{4E}/m}, \tag{20}$$

where

$$I(\vec{p},\vec{p}';E) = \int_0^1 \rho^{i\eta}\left[\rho(\vec{p}-\vec{p}')^2 - \frac{m}{4E}(E-T)(E-T') \times (1-\rho)^2\right]^{-1} d\rho.$$

In our case we obtain

$$t_{pp}\left[\frac{\vec{p}+\vec{q}'}{2},\frac{\vec{p}-\vec{q}'}{2}+\vec{q};\frac{p^2}{4m}+E_0^{\mathrm{H}}+\frac{\vec{v}_p\vec{q}'}{2}-\frac{q'^2}{2}+i0\right]$$
$$\approx 4\pi\left[\frac{1}{(\vec{q}-\vec{q}')^2}-\frac{i}{v_p}\int_0^1\frac{\rho^{i/v_p}\,d\rho}{[\rho(\vec{q}-\vec{q}')^2-v_p^{-2}(E_0^{\mathrm{H}}-q'^2/2)[E_0^{\mathrm{H}}-(\vec{v}_p-\vec{q}')^2/2](1-\rho)^2+i0]}\right].$$

The integral $F_3$ takes the form

$$F_3 = A_3 - \Delta A_3, \tag{21}$$

where

$$\Delta A_3 = \frac{4\pi i}{v_p}\int_0^1 d\rho\,\rho^{i/v_p}\int\frac{d^3\vec{q}'}{(2\pi)^3}\frac{\varphi_0(q')\varphi(\vec{v}_p-\vec{q}')}{[\rho(\vec{q}-\vec{q}')^2-v_p^{-2}(E_0^{\mathrm{H}}-q'^2/2)[E_0^{\mathrm{H}}-(\vec{v}_p-\vec{q}')^2/2](1-\rho)^2+i0]}. \tag{22}$$

As one can see in Fig. 6 the divergence between B1 and B1F results is noticeable only in the gap region $\theta \sim 0.3-0.4$ mrad.

It is impossible to take fully into account the two-body amplitudes $t_{pp}$ and $t_{ep}$ in the numerical B2F calculation, although there are analytical expressions for these amplitudes [20]. We suppose that $t_{pp}=V_{pp}$. Such a proposal is based on the calculations of integral (22). Futher, the operator $t_{ep}$ can be presented in the form

$$t_{ep}(E) = V_{ep} + \sum_s \frac{V_{ep}|\varphi_s\rangle\langle\varphi_s|V_{ep}}{E-\varepsilon_s+i0}, \tag{23}$$

where $|\varphi_s\rangle$ is a full orthonormal set of the Coloumb eigenfunctions of the two-body problem. In the closure approximation (CA) the eigenenergy is replaced by an averaged value $\epsilon_s \to \overline{E}$. In this case from Eq. (23) the following expression can be obtained:

$$\langle\vec{p}'|t_{ep}(E)|\vec{p}\rangle = -\frac{4\pi}{(\vec{p}'-\vec{p})^2}+\frac{1}{8}\frac{(4\pi)^2}{E-\overline{E}+i0}\frac{1}{|\vec{p}'-\vec{p}|}, \tag{24}$$

where $\overline{E}$ is the CA parameter, $-0.5 \leqslant \overline{E} < 0$. This means that we consider here only an averaged contribution of bound excitations to the $(ep)$ amplitude.

After taking into account $t_{ep}$ in the form (24) and carring out some transformations of the integrals the correction to the B2 result looks like

$$I = \frac{1}{\pi^3}\int\int\frac{d^3\vec{x}}{x}\frac{d^3\vec{y}}{y^2}\frac{\varphi_0(\vec{v}_p-\vec{q}+\vec{y})}{(1+2\overline{E})+2\vec{v}_p\vec{y}-i0}$$
$$\times\frac{[\varphi_0(\vec{q}-\vec{x}-\vec{y})-\varphi_0(\vec{q}-\vec{x})]}{1+2\vec{v}_p\vec{y}+(\vec{q}-\vec{x}-\vec{y})^2-i0}. \tag{25}$$

Thus the B2F amplitude of the problem in our approximation assumes the form $T_{B2F}=A_1+F_3+A_{11}+A_{31}+A_{13}+I$. The convoluted results of these calculations are presented in Fig. 7. The best fitting is reached at $\overline{E}=-0.4$. The calculations in the B2 and FWL [17] approximations are also presented for the completeness.

Two important conclusions follow from comparison of the curves. The first is that one can see the instability of the contribution of the $(ep)$ excitations (a distortion of the waves) with growth of the proton energy. This contribution is relatively small in the whole angular range at $E_p=2.8$ MeV. But at $E_p=5.0$ MeV this contribution is sufficiently big at $\theta_p=0.2-0.5$ mrad. At the same time we see that the B2F model approaches the experiment at $E_p=2.8$ MeV and practically coincides in the angular range $\theta_p=0-0.25$ mrad. In the angular range $\theta_p=0.25-0.5$ one can see the discrepancy between the theoretical and experimental results. We ascribe this effect to the necessity to take more carefully into account the $(ep)$ pair continuum intermediate states.

Comparison between the B1F calculations and the first-order FWL model calculations is also presented in Fig. 8, where (as we mentioned in the Introduction) the two-body Coulomb amplitudes $t_C$

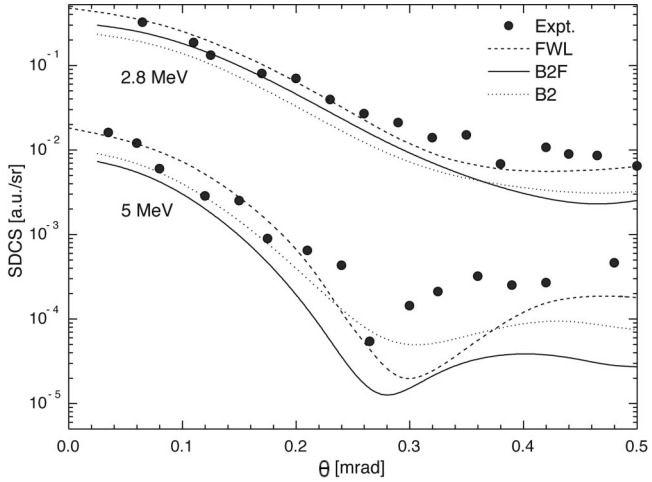


FIG. 7. Differential cross sections for $1s \to 1s$ capture in 2.8 and 5.0 MeV proton-hydrogen collisions vs the scattering angle in the laboratory system. Results of B2F (solid line), FWL (dashed line, Ref. [17]), and B2 (dotted line) calculations are compared with the experimental data of Vogt (Ref. [5]). All theoretical results have been convoluted with the beam profiles.

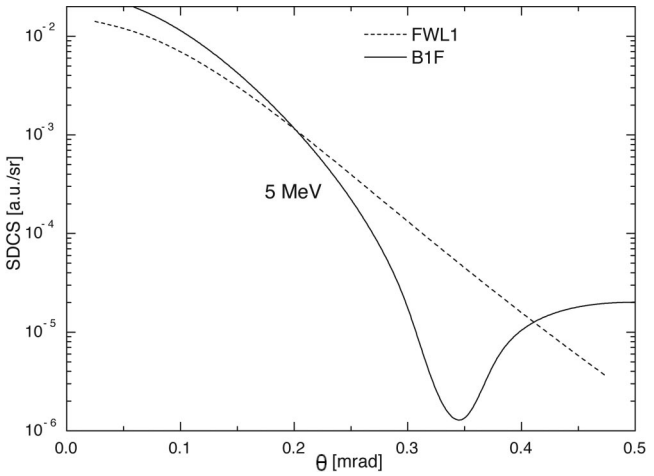


FIG. 8. Test of the accuracy of the first-order FWL model. Results of FWL1 (dashed line) and B1F (solid line) calculations are compared.

$$t_C(\vec{k}',\vec{k};\varepsilon) = \langle \vec{k}' | V_C \left( 1 + \left[ \varepsilon - \frac{1}{2\mu}\nabla_r^2 - V_C + i\eta \right]^{-1} V_C \right) | \vec{k} \rangle \times (C = pp, ep) \tag{26}$$

in the vertices of $F_3$, $F_{13}$, $F_{31}$, and $F_{11}$ diagrams are taken only in a limited neighborhood of the energy shell, when

$$\delta = \frac{(2\mu E - k^2)(2\mu E - k'^2)}{2\mu E |\vec{k} - \vec{k}'|^2} \ll 1.$$

Such an approximation contains a number of "submarine reefs," because the amplitude $t_C(\vec{k},\vec{k}';E)$ is a formally singular function in this neighborhood [21]. Moreover, after this substitution Alston calculates the resulting multidimensional integrals in the peaking approximation. Many authors mentioned that the peaking approximation is rather crude at moderate energies, and we see that the numerical and approximate B2 calculations considerably differ from each other. To test the accuracy of the FWL model, the first-order calculations within this model (FWL1 $= A_{B1} + A_n^{(1)}$; see Eq. (33) in [17]) were performed and compared with the precise calculations of the term B1F. As can be seen in Fig. 8, in this case the FWL model demonstrates very poor convergency to the precise calculations.

## IV. SUMMARY

We present here precise numerical calculations of the plane wave B1 and B2 terms for the proton-hydrogen charge exchange reaction at small scattering angles and moderate energies of existing experiments. The obtained results clearly show the considerable role of double-scattering mechanisms even in the angular range 0–0.1 mrad. In any case the term $A_1$ = B1E [Eq. (17)], which contains the direct information on the ground state wave function, can be dominant nowhere (see Fig. 3). This observation means that the charge exchange reaction at small scattering angles (with or without ionization of the residual ion) cannot be effectively used for the angular spectroscopy of a target's correlation structure.

We also can formulate the following conclusions.

(1) The performed numerical calculation of the multiple integrals describing the B2 matrix elements shows that the peaking approximation is rather crude and can be used only for general estimates of differential cross sections at small hydrogen scattering angles and high energies of actual experiments. One finds a slow convergence between precise and approximate calculations with growth of the proton energy.

(2) The widely known thesis that the B2E contribution is dominant in the total second Born approximation ($|A_1 + A_{11}| \gg |A_3 + A_{13} + A_{31} + A_{33}|$) is valid only for the peaking approximation at high energies. Numerical calculations at moderate energies give the opposite result. Figure 3 clearly demonstrates that there is no complete cancellation of the terms containing the internuclear potential.

(3) In the B1 minimum region ($\theta_p \sim 0.3$ mrad) a number of factors affect the cross-section behavior. One should take into account ($ep$) subsystem excitations into discrete and continuum spectra, proton-nuclear scattering, and even the accuracy of the hydrogen final-state measurements [8].

(4) We also present here numerical calculations of the effects of the wave distortion which naturally reveal themselves by means of intermediate two-body Coulomb amplitudes. This distortion effect is quite small for protons, which is to be expected in the considered angular domain. The distortion of electron waves becomes apparent in the Thomas peak region ($\theta_p \geqslant 0.4$ mrad). However, the simple models, such as the closure or eikonal approximations, do not yield the desired results. The accurate representation models of the two-body amplitude $t_{ep}$ [Eq. (26)] appropriate for numerical calculations must be involved in the whole range of variation of its three arguments. This problem is the most difficult in spite of the analytical form of this amplitude.

(5) Finally, we estimate numerically the effect of motion of the proton in the final state which initially was at rest in the laboratory system. We found it to be practically negligible as it should be in the considered domains of angles and energies.

## ACKNOWLEDGMENTS

We are grateful to R. Rivarola, A. Martinez, and R. Schuch for their help in the solution of the convolution problem. P.S.V. would like to thank the Dynasty Foundation for partial financial support of this work. One of us (Yu.P.) is grateful to H. Shmidt-Böking for motivating these investigations and his hospitality in Frankfurt. This work is partially supported by the foundation "Universities of Russia."

## APPENDIX A: FIRST-ORDER TERM

Let us consider the first-order matrix element $A_3$

$$A_3 = 4\pi \int \frac{d^3\vec{q}'}{(2\pi)^3} \varphi_0(q') \frac{1}{(\vec{q} - \vec{q}')^2} \varphi(\vec{v}_p - \vec{q}').$$

After the replacement $\vec{q} - \vec{v}_p + \vec{q}' = \vec{k}$ and double Laplace transformations it reads

$$A_3 = \frac{32}{\pi}\int_0^\infty t_1\,dt_1\int_0^\infty t_2\,dt_2\int\frac{d\vec{k}}{k^2}\exp(-\{[1+(\vec{q}-\vec{k})^2]t_1 + [1+(\vec{k}-\vec{q}+\vec{v}_p)^2]t_2\})$$
$$= 64\sqrt{\pi}\int_0^\infty t_1\,dt_1\int_0^\infty t_2\,dt_2 \times\frac{\exp\{-(q^2+1)t_1-[1+(\vec{v}_p-\vec{q})^2]t_2\}}{\sqrt{t_1+t_2}} \times{}_1F_1\left(\frac{1}{2},\frac{3}{2};\frac{[\vec{q}t_1-(\vec{v}_p-\vec{q})t_2]^2}{t_1+t_2}\right).$$

We put $t_1=\rho x$, $t_2=\rho(1-x)$,

$$A_3 = 64\sqrt{\pi}\int_0^1 x(1-x)dx\int_0^\infty d\rho\,\rho^{5/2}\exp\{-\rho[(q^2+1)x - (\vec{v}_p-\vec{q})^2+1](1-x)\}{}_1F_1\left(\frac{1}{2},\frac{3}{2};\rho[\vec{q}-\vec{v}_p(1-x)]^2\right).$$

The integral over $\rho$ can be calculated analytically, and finally we obtain

$$A_3 = 120\pi\int_0^1\frac{x(1-x)}{\beta^{7/2}}{}_2F_1\left(\frac{7}{2},\frac{1}{2};\frac{3}{2};\frac{\lambda}{\beta}\right) = 120\pi\int_0^1 dx\frac{x(1-x)[1+2\lambda/3(\lambda-\beta)+\lambda^2/5(\lambda-\beta)^2]}{[\beta-\lambda]^{1/2}[\beta]^3}dx,$$

where $\beta=[(q^2+1)x-(\vec{v}_p-\vec{q})^2+1](1-x)$, $\lambda=[\vec{q}-\vec{v}_p(1-x)]^2$.

## APPENDIX B: SECOND-ORDER TERM

We consider here the second-order matrix element $A_{11}$ as an example. The following chain of transformations can be applied:

$$A_{11} = (4\pi)^2\int\frac{d^3q'}{(2\pi)^3}\int\frac{d^3q''}{(2\pi)^3}\varphi_0(q') \times\frac{1}{q''^2}\frac{1}{E_0^{\mathrm{H}}-\vec{v}_p\vec{q}''-(\vec{q}'-\vec{q}'')^2/2+i0}\frac{1}{(\vec{q}'-\vec{q})^2} \times\varphi_0(\vec{v}_p+\vec{q}''-\vec{q}),$$

$$A_{11} = \frac{32}{\pi^3 i}I_{11},\quad I_{11} = \int\frac{d^3x}{(\vec{q}-\vec{x})^2}\frac{1}{(1+x^2)^2}\int_0^\infty\int_0^\infty t_1\,dt_1\,dt_3\,J_1,$$

$$J_1 = \int\frac{d^3y}{y^2}\exp(-y^2(it_3+t_1)+2\vec{y}[it_3\vec{x}-it_3\vec{v_p}-t_1(\vec{v_p}-\vec{q})] - \{it_3(1+x^2)+t_1[1+(\vec{v_p}-\vec{q})^2]\}) = \frac{2\pi^{3/2}}{\sqrt{t_1+it_3}}{}_1F_1\left(\frac{1}{2},\frac{3}{2};\frac{(it_3\vec{x}-it_3\vec{v_p}-t_1(\vec{v_p}-\vec{q}))^2}{t_1+it_3}\right) \times\exp(-\{it_3(1+x^2)+t_1[1+(\vec{v_p}-\vec{q})^2]\}),$$

$${}_1F_1\left(\frac{1}{2},\frac{3}{2};\frac{[it_3\vec{x}-it_3\vec{v_p}-t_1(\vec{v_p}-\vec{q})]^2}{t_1+it_3}\right) = \frac{1}{2}\int_0^1\frac{du}{\sqrt{u}}\exp\left(u\frac{[it_3\vec{x}-it_3\vec{v_p}-t_1(\vec{v_p}-\vec{q})]^2}{t_1+it_3}\right).$$

Let us replace $\vec{x}\to\vec{x}+\vec{q}$ and note that $(\vec{v}_p-\vec{q})^2=q^2$. Then

$$I_{11} = 2\pi^{3/2}\int_0^1\frac{du}{\sqrt{u}}\int_0^\infty\int_0^\infty\int_0^\infty\frac{t_1t_2\,dt_1\,dt_2\,dt_3}{\sqrt{t_1+it_3}}J_2,$$

$$J_2 = \int\frac{d^3x}{x^2}\exp\left[-x^2\left(t_2+it_3+\frac{ut_3^2}{t_1+it_3}\right) - 2\vec{x}[t_2\vec{q}+it_3\vec{q}+u(\vec{v}_p-\vec{q})it_3]\right] \times\exp(-\{t_2(1+q^2)+it_3(1+q^2) + t_1[1+(\vec{v}_p-\vec{q})^2]-u(t_1+it_3)q^2\}) = \frac{2\pi^{3/2}}{\sqrt{t_2+it_3+ut_3^2/(t_1+it_3)}} \times{}_1F_1\left(\frac{1}{2},\frac{3}{2};\frac{[t_2\vec{q}+it_3\vec{q}+u(\vec{v}_p-\vec{q})it_3]^2}{t_2+it_3+ut_3^2/(t_1+it_3)}\right) \times e^{-[(t_1+t_2+it_3)(1+q^2)-u(t_1+it_3)q^2]}.$$

We designate $t_1=\rho xy$, $t_2=\rho(1-x)y$, $t_3=\rho(1-y)$, and after integrating by $\rho$ we obtain

$$I_{11} = 24\pi^3\int_0^1\int_0^1\int_0^1\frac{y^3x(1-x)dx\,dy\,du}{\sqrt{u}\sqrt{(l_1+il_3)(l_2+il_3)+ul_3^2}}\frac{1}{\beta^4} \times{}_2F_1\left(4,\frac{1}{2};\frac{3}{2};\frac{\lambda}{\beta}\right),$$

where $l_1=xy$, $l_2=(1-x)y$, $l_3=(1-y)$, and

$$\beta = (l_1+l_2+il_3)(1+q^2)-u(l_1+il_3)q^2,$$

$$\lambda = \frac{[l_2\vec{q}+il_3\vec{q}+u(\vec{v}_p-\vec{q})il_3]^2}{l_2+il_3+ul_3^2/(l_1+il_3)},$$

$${}_2F_1\left(4,\frac{1}{2};\frac{3}{2};z\right) = \frac{1}{96}\left[\frac{16}{(1-z)^3}+\frac{20}{(1-z)^2}+\frac{30}{(1-z)} + \frac{15}{\sqrt{z}}\ln\left(\frac{1+\sqrt{z}}{1-\sqrt{z}}\right)\right].$$

[1] Dz. Belkić, R. Gayet, and A. Salin, Phys. Rep. **56**, 281 (1979).
[2] V. M. Lendiel, Yu. V. Lazur, M. I. Karbovanetz, and R. K. Yanev, *Introduction to the Theory of the Atomic Collisions* (Vischa Shkola, Lvov, 1989).
[3] V. Mergel, Ph.D. thesis, University of Frankfurt/Main, Germany, 1996; V. Mergel, R. Dörner, M. Achler, Kh. Khayyat, S. Lencinas, J. Euler, O. Jagutzki, S. Nüttgens, M. Unverzagt, L. Spielberger, W. Wu, R. Ali, J. Ullrich, H. Cederquist, A. Salin, C. J. Wood, R. E. Olson, Dz. Belkić, C. L. Cocke, and H. Schmidt-Böcking, Phys. Rev. Lett. **79**, 387 (1997); V. Mergel, R. Dörner, Kh. Khayyat, M. Achler, T. Weber, O. Jagutzki, H. J. Lüdde, C. L. Cocke, and H. Schmidt-Böcking, *ibid.* **86**, 2257 (2001).
[4] Yu. V. Popov, O. Chuluunbaatar, S. I. Vinitsky, L. U. Ancarani, C. Dal Capello, and P. S. Vinitsky, JETP **95**, 620 (2002).
[5] H. Vogt, R. Schuch, E. Justiniano, M. Schulz, and W. Schwab, Phys. Rev. Lett. **57**, 2256 (1986); H. G. Vogt, Ph.D. thesis, University of Heidelberg, Germany, 1986.
[6] I. M. Cheshire, Proc. Phys. Soc. London **84**, 89 (1964).
[7] J. E. Miraglia, R. D. Piacentini, R. D. Rivarola, and A. Salin, J. Phys. B **14**, L197 (1981).
[8] H. F. Busnengo, A. E. Martinez, R. D. Rivarola, and L. J. Dube, J. Phys. B **28**, 3283 (1995).
[9] L. H. Thomas, Proc. R. Soc., London, Ser. B **114**, 561 (1927).
[10] J. S. Briggs and K. Taulbjerg, J. Phys. B **12**, 2565 (1979); S. G. Tolmanov and J. H. McGuire, Phys. Rev. A **62**, 032711 (2000).
[11] P. R. Simony and J. H. McGuire, J. Phys. B **14**, L737 (1981).
[12] H. L. Kyle and M. R. C. McDowell, J. Phys. B **2**, 15 (1969).
[13] M. R. C. McDowell and J. P. Coleman, *Introduction to the Theory of Ion-Atom Collisions* (North-Holland, Amsterdam, 1970).
[14] L. D. Faddeev and S. P. Merkuriev, *Quantum Scattering Theory for Several Particle Systems* (Kluwer Academic, Dordrecht, 1993).
[15] V. V. Komarov and A. M. Popova, Nucl. Phys. **54**, 278 (1964); **69**, 253 (1965); Nucl. Phys. A **90**, 625 (1967).
[16] A. M. Brodsky, V. S. Potapov, and V. V. Tolmachev, Sov. Phys. JETP **31**, 144 (1970).
[17] S. Alston, Phys. Rev. A **42**, 331 (1990).
[18] S. Alston, Phys. Rev. A **38**, 6092 (1988).
[19] E. Ghanbari Adivi and M. A. Bolorizadeh, J. Phys. B **37**, 3321 (2004).
[20] C. S. Shastri, L. Kumar, and J. Callaway, Phys. Rev. A **1**, 1137 (1970); C. S. Shastry and A. K. Rajagopal, *ibid.* **2**, 781 (1970).
[21] J. Schwinger, J. Math. Phys. **5**, 1606 (1964).